1. Md Mainul ISLAM[1], 2. Hussain SHAREEF[2] 3. Eslam Salah Fayez Al HASSAN[3]

Western Sydney University (1), United Arab Emirates University (2,3)
ORCID: 1. 0000-0002-8079-2065; 2. 0000-0001-7708-6904; 3. 0000-0002-4909-5106; 4. 0000-0002-1401-0280

doi:10.15199/48.2023.04.27

Deep Learning Technique for Forecasting Solar Radiation and Wind Speed for Dynamic Microgrid Analysis

Abstract. *The key variables in the development and operation of wind and solar power systems are wind speed and solar radiation. The prediction of solar and wind energy parameters is important to alleviate the effects of power generation fluctuations. Consequently, it is essential to predict renewable energy sources like solar radiation and wind speed precisely. An artificial intelligence-based random forest method is recommended in this paper to estimate wind speed and solar radiation. The number of decision trees in the random forest model is suggested to be optimised using a novel coot algorithm (CA), and the effectiveness of the CA is evaluated to that of the currently used particle swarm optimisation (PSO) method. The best forecasting data are used in this work to develop a dynamic Microgrid (MG) in MATLAB/SIMULINK. A novel binary CA is proposed to control the MG to minimize the cost. The effect of the energy storage system is also investigated during the simulation of the MG.*

Streszczenie. *Kluczowymi zmiennymi w rozwoju i działaniu systemów energii wiatrowej i słonecznej są prędkość wiatru i promieniowanie słoneczne. Prognozowanie parametrów energii słonecznej i wiatrowej jest ważne dla złagodzenia skutków wahań produkcji energii. W związku z tym niezbędne jest precyzyjne przewidywanie źródeł energii odnawialnej, takich jak promieniowanie słoneczne i prędkość wiatru. W tym artykule zaleca się metodę lasów losowych opartą na sztucznej inteligencji w celu oszacowania prędkości wiatru i promieniowania słonecznego. Sugeruje się optymalizację liczby drzew decyzyjnych w modelu losowego lasu przy użyciu nowego algorytmu łyski (CA), a skuteczność CA jest oceniana na podstawie obecnie stosowanej metody optymalizacji roju cząstek (PSO). W tej pracy wykorzystano najlepsze dane prognostyczne do opracowania dynamicznej mikrosieci (MG) w MATLAB/SIMULINK. Proponuje się nowy binarny CA do sterowania MG w celu zminimalizowania kosztów. Wpływ systemu magazynowania energii jest również badany podczas symulacji MG.* (***Technika głębokiego uczenia się do prognozowania promieniowania słonecznego i prędkości wiatru na potrzeby dynamicznej analizy mikrosiec***i)

Keywords: Solar power, wind power, random forest method, coot algorithm, microgrid, forecasting.
Słowa kluczowe: energia słoneczna, energia wiatrowa, prognozowanie, głębokie uczenie

1. Introduction

Governments and legislators have been pushed to find and employ alternative energy supplies throughout the past few decades as a result of environmental concerns and a lack of energy. It would make it easier to take over the current electricity generation [1, 2]. The use of RESs, such as solar and wind energy, is something the researchers are interested in doing to prevent power outages and significantly lower carbon dioxide discharges. RESs have shown tremendous market growth in upcoming years and are now a globally viable source of power for pricing. RESs will deliver 2/3 of the world's energy demand by 2050 [3]. How to integrate this sporadic energy source into the smart power grid is the apparent obstacle in the RES industry's sustained growth [4]. For substantial energy production, wind and solar plants need consistent, appropriate wind speed and sun irradiation [5]. For dependability, utility, simplicity, and multiple-purpose applicability, an accurate solar and wind speed forecast approach is required [6, 7]. Due to its dependence on several atmospheric characteristics, the prediction of RESs is both an important and difficult topic. The forecast error has a major damaging impact on the power system's economic and productive performance. [8].

Over the past few decades, various forecasting techniques have been used to address the RESs forecasting issue. Each strategy has particular advantages and implementation requirements. Direct and indirect forecasts are two categories into which the forecasting techniques can be separated. The earlier techniques used historical power data to predict solar and wind energy output. Nevertheless, the latter tactics estimate solar irradiance, wind speed, and additional meteorological parameters first before converting them to power generation by taking into account the PV and wind system characteristics. Through least-squares optimisation, the authors developed an indirect forecast method for day-ahead solar power. The numerical weather forecast model used to determine solar irradiation is available to the general public [9]. Using the data from the day before, the authors forecast the hourly sun irradiance for the following day [10]. The prediction approach employed was a backpropagation neural network (NN). Jiang created an artificial NN system using a feed-forward back-propagation technique to estimate day-to-day sun radiation [11]. To predict mean worldwide sun irradiation, the authors developed a statistical regression methodology, and the efficacy of the proposed method was assessed using various statistical indicators [12]. The authors proposed a time-series regression for estimating solar radiation with an autoregressive integrated moving average (ARIMA) method [13]. Short-term solar irradiance forecasting was done by Yang et al. using a lasso linear regression method [14]. Using data on American sun irradiation, a detailed evaluation was carried out. According to the outcomes, lasso linear regression outperforms both standard linear regression and ARIMA models. For estimating solar irradiation one hour in advance, Ref. [15] suggested a novel hybrid deep neural approach. To extract data features, a decoupling procedure is first used to divide the relevant historical data into several intervals of time series. Second, to predict solar irradiance, a deep-learning network incorporating a convolution neural network (NN) and a long short-term memory (LSTM) is utilized.

Ref [16] suggested a novel hybrid Elman NN model to improve wind speed predicting outcomes. To keep the model's variance low while maintaining the anticipated outcomes' accuracy and stability, a multi-objective optimisation technique is used. To overcome the shortcomings of the Elman NN, the proposed model incorporated an adaptive wind-driven optimisation approach and a modified simulated annealing approach. A wind speed bi-forecasting method with data pre-processing, combination forecasting, and evaluation was put forth by Nie et al. [17]. To create a time series and get rid of high-frequency noise components, a decomposition method is used to accomplish decomposition and reconstruction of the true wind speed. The weight combination technique was

adopted in the combined forecasting strategy, which relied on a multi-verse optimisation process to produce a dual outcome of forecasting. Similar to this, Lie et al. proposed a novel hybrid data separation and deep learning NN model-based wind speed forecasting system [18]. The system is made up of modules for data preprocessing, forecasting, and extraction. The wind speed input is divided into various time series periods using a decomposition approach after being taken from a sizeable amount of original historical data. The LSTM forecast module is enhanced using a genetic algorithm, which is then combined for producing the final forecast results. The hybrid models' drawback is the complexity of the problems they can formulate. By using a support vector machine method for the error in prediction, a spot forecast of wind generation was conducted by Yang et al. [19]. The authors in [20] used a neural network with a covariance adaption evolutionary approach to successfully forecast wind generation. To predict the wind speed to install a wind power plant, the authors used the ARIMA technique with wavelet transform [13]. Ref. [21] provided a succinct overview of renewable energy, measuring techniques, and forecasts of solar radiation and wind speed for effective use of RESs.

To create a microgrid (MG) and deliver enough energy to satisfy consumer demand, RESs are gathered. The adoption of distributed generators powered by renewable resources keeps growing. Diverse MG installations offer important benefits such as access to comprehensive distributed generator integration, efficiency enhancement, cost, risk, and pollution reduction. However, MGs also present some difficulties. For instance, because standard tactics are unable to continually adapt to MGs' dynamic behaviour, new energy management and control strategies are required Controlling is crucial in an MG scheme to provide customers with higher-quality, more dependable, and sustainable energy [23]. To account for geothermal and biomass generators, solar energy, and battery storage systems, Ignat et al. constructed an MG in MATLAB/SIMULINK [24]. Data on the weather is sourced from a NASA database. An operating cost optimisation algorithm simulates the MG. To reduce operational costs, Abdolrasol et al. created an MG in MATLAB/SIMULINK by integrating a virtual power plant [25]. The best scheduling controller is advised to use a binary backtracking search technique. An MG was created in [26] to maximise the employment of local RES and decrease operational costs, just as in earlier studies. The MG Simulink model is simulated using the HOMER software. For the efficient operation of an MG and the control of energy, numerous optimisation techniques and heuristics have been used [27-30].

To generate renewable energy, a variety of methods have been used to anticipate solar radiation and wind speed. Prediction models now in use are appropriate for specific activities, locales, or applications. To predict both wind speed and sun radiation simultaneously, very few models are created. Furthermore, not all problems can be accurately predicted using a single prediction method. To forecast wind speed and solar radiation, the author suggests using a random forest (RF) method that is based on deep learning [31]. The key problem of the suggested strategy is the right choice of leaves and trees for the RF model. To choose the right number of decision trees that can reduce forecasting mistakes, the innovative coot algorithm (CA) is suggested [32]. When compared to the particle swarm optimisation (PSO) method, the proposed CA strategy performs better. Additionally, a novel binary CA known as BCA is recommended for MG energy management created in MATLAB/SIMULINK. The MG model uses the RF-based optimal forecasted data as its source.

The following is the research's primary contribution:

1. To forecast solar irradiation and wind speed, a random forest technique based on deep learning is suggested.
2. To preserve accuracy, the decision trees are optimised using a cutting-edge optimisation method known as the coot algorithm.
3. Using the data from the day-ahead anticipated solar irradiance and wind speed, a dynamic microgrid is created in MATLAB/SIMULINK.

The paper is structured as follows Section 2 presents wind speed and solar irradiance forecasting. Section 3 describes the model for forecasting. Section 4 provides an illustration of the microgrid model. Section 5 presents the simulation findings, while Section 6 draws conclusions.

2. Prediction of wind speed and solar radiance

The correct choice of input parameters and the prediction timeline determine the forecasting model's accuracy. In the microgrid and smart grid, many forecasting horizons reflect to the various requirements of decision-making actions [33]. The focus of the ongoing study is on developing a day-ahead prediction approach.

2.1. Data collection and processing

For day-ahead forecasting, historical information on wind speed and sun radiation is crucial. The Australian Bureau of Meteorology provides daily statistics on variables such as station pressure, mean ambient air temperature, wind speed, solar radiation, relative humidity, and others [34]. Before the training phase all inputs and the target are normalised to the interval [0,1] using equation (1) [35]. The normalised data can speed up training and assist in preventing overflow calculations.

$$\overline{X} = \left\{ \frac{X_k - X_{\min}}{X_{\max} - X_{\min}} \right\}; \quad 0 \le \overline{X} \le 1 \tag{1}$$

where $\bar{X}$ represents the normalized value of data X_k; X_{min} and X_{max} are the minimum and maximum values of X_k. After the normalisation procedure is complete, the entire dataset is divided into 2 sub-sets, namely the training data and the testing data. About 70% of the dataset for each of them are utilised for training. The remaining 30% is utilized for testing. To prevent the data from reoccurring, great caution is taken.

2.2. Performance evaluation

In this work, the effectiveness of the soft computing strategy is measured using statistical indices such as root-mean-square error (RMSE) and mean absolute percentage error (MAPE). The indices' mathematical expression is as follows [36]:

$$MAPE = \frac{1}{N} \sum_{n=1}^{N} \frac{| M_j - P_j |}{M_j} \times 100\% \tag{2}$$

$$RMSE = \sqrt{\frac{1}{N} \sum_{n=1}^{N} (M_j - P_j)^2} \tag{3}$$

where N is the number of samples, M_j and P_j are measured and predicted values.

3. Forecasting model

3.1. Random forest (RF)

RF during training creates a huge number of decision trees and classifies or predicts the mean value of each tree (regression) [31]. Classification and regression issues, which comprises the majority of modern machine learning

systems, are where RF excels. The RF addresses the issue that decision trees frequently overfit a given training set. The bootstrapping aggregating method is a common way to train tree learners in the training operation of RF. The RF predicts or classifies the value of a variable for an input vector m, by building several regression trees K. Further, it averages the results as shown in Fig.1. It is possible to express the RF regression predictor as

(4) $$f_{RF}^{K} = \frac{1}{K}\sum_{i=1}^{K} T(m)$$

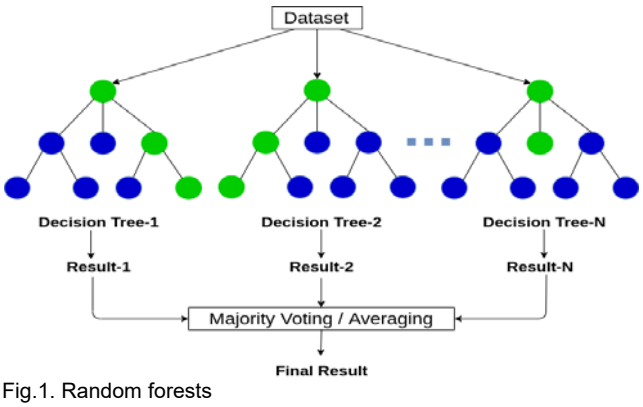

Fig.1. Random forests

Regression using the RF technique operates as follows [37]:

1. The bootstrap samples are generated at random using replacements from the main dataset, and each sample contains around 2/3 of the training dataset. The RFs model is constructed for each sample using unique patterns from the dataset. The data that can be used for testing but was removed from the learning sample is known as "out-of-bag" (OOB) dataset.
2. To establish the binary rule, a subset of the predictor parameters is randomly nominated at each regression tree node. Depending on the residual sum of squares (SoS), the variable is preferred. For the split, the predictor with the lowest residual SoS is selected.
3. The maximum amount of development has been done to each sample tree. The tree isn't pruned at all.
4. As a final step, predictions are made for each of the sample trees by looking at the test data. The final anticipated estimate is derived by averaging the predictors from each regression tree.

The OOB error, or mean square error, is calculated using the differences between reference and forecast values. Performance is measured using these OOB error items.

3.2. Optimization technique for random forest

If there are a lot of training data and decision trees, the RF approach may predict error-free parameters. The algorithm becomes more difficult as more data and decision trees are used. Thus, the parameter approximation is required to achieve the output that is the greatest degree of similarity to the observed data as possible with the least amount of error. Utilizing the smallest amount of errors, the CA is used to optimise the quantity of decision trees.

3.2.1. Coot algorithm

The Coot algorithm (CA), a revolutionary meta-heuristic optimisation method derived from the small water birds of the rail family. The optimisation process is put into practise by accounting for the 4 coot activities on the water's surface.

a) Random activity

To perform this movement, equation (5) is first used to generate a random coot position in the search space.

(5) $$P = rand(1,m).*(ub - lb) + lb$$

where *lb* and *ub* represents lower and upper limits, *m* is the number of dimensions.

The coot changes positions inside the search area. The algorithm can escape the local optimal thanks to this mobility. Equation (6) is used to formulate coot's new position.

(6) $$Cpos(k) = Cpos(k) + A \times rand \times (P - Cpos(k)$$

where *A* is calculated based on equation (7).

(7) $$A = 1 - iter \times (\frac{1}{MaxIter})$$

where *MaxIter* and *iter* are the maximum and current iterations.

b) Chain activity

The normal position of 2 coots is used to compute the chain activity. Based on equation (8), the coot's new location is determined.

(8) $$Cpos(k) = 0.5(Cpos(k-1) + Cpos(k))$$

where *Cpos(k-1)* is the previous (second) coot

c) Position modification considering the group leaders

The other coots modify their positions in accordance with the average position of the group leaders after taking it into account. The formula (9) is used to choose the leader

(9) $$D = 1 + (kMODL)$$

where *L* is the number of leaders, *D* and *k* represent the leader and the index number of the current coot respectively.

Equation (10) is used to determine the coot's next position after the best leader.

(10) $$Cpos(k) = Lpos(d) + 2 \times rand \times cos(2R\pi) \times (Lpos(d) - Cpos(k))$$

where *R* is the random numbers [-1,1].

d) Leader activity

Equation (11) is used to assess the leaders' locations to determine the best position.

(11) $$pos(k) = \begin{cases} B \times rand \times cos(2R\pi) \times (pBest - Lpos(k)) + pBest & rand < 0.5 \\ B \times rand \times cos(2R\pi) \times (pBest - Lpos(k)) - pBest & rand >= 0.5 \end{cases}$$

Where *pBest* is the best global location and B is obtained using equation (12)

(12) $$B = 2 - iter \times (\frac{1}{MaxIter})$$

3.3. Random forest implementation

The following variables are used as inputs for estimating solar radiation: latitude, longitude, mean relative humidity, air temperature and time. Similar to this, the inputs of weather temperature, time and pressure are utilised to forecast the outputs of solar radiance and wind speed. Figure 2 shows a simplified diagram of the RF method.

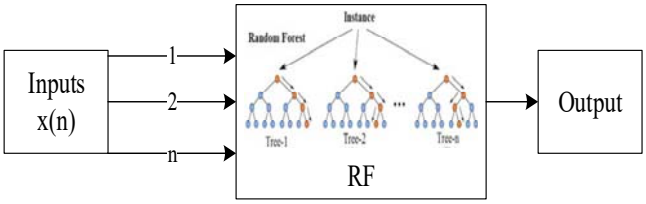

Fig.2. The schematic illustration of RF approach

The RF prediction method consists of three steps. The initial part of the data collection is receiving the collected data, and the middle stage is processing it using CA to establish the quantity of decision trees. The calculated information is provided in the last stage. By training a large amount of input/output data, it is possible to anticipate the output value of an RF structure. The CA technique is used to optimise the suggested RF model and forecast the output parameter with the least amount of inaccuracy. By contrasting the CA's performance with that of the well-known PSO algorithm, its performance is confirmed. Fig. 3 depicts the CA flowchart for optimising the RF model.

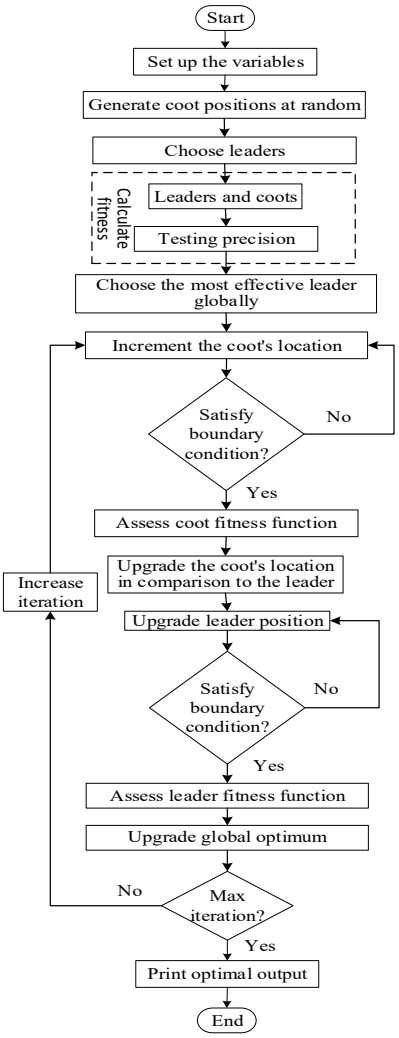

Fig.3. CA flowchart for RF optimization

4. Microgrid model

4.1. Microgrid model in Simulink

The dynamic MG consists of a diesel generator, PV farm, wind farm, battery storage and residential load. Diesel generator act as the primary power source and PV and wind plants are used to produce renewable energy. The best-forecasted data of solar radiance and wind speed from the CA-based RF are utilized as inputs for PV and wind farms in MATLAB/SIMULINK. The power generation from the PV farm relies on the area of the farm, predicted solar irradiance data and the efficiency of the PV panel. The wind farm generates electrical power based on a linear relationship with the predicted wind speed. The wind farm cannot generate electricity when the wind speed outstrips the speed limitations (beyond 7 to 15 m/s). Fig.4 shows the Simulink model of MG utilized in this research work.

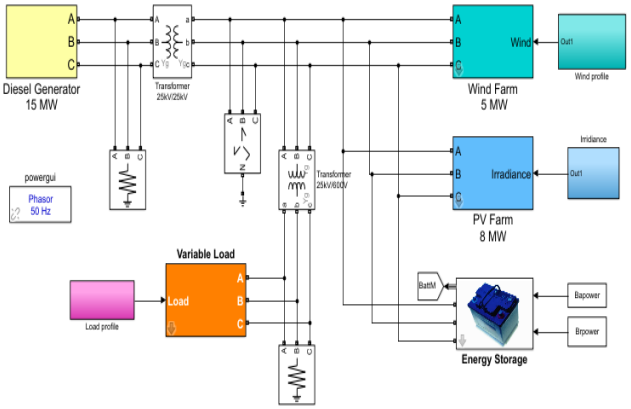

Fig.4. Simulink model of dynamic MG

4.2. Binary Coot Algorithm

The novel CA only works for the continuous-based problem. However, a binary algorithm is expected to control (on/off) the MG for minimizing the operating cost. In this study, a binary CA (BCA) is developed whose search surface is limited to [0,1]. The activity of the coot in the search surface is updated by changing the position between '0' and '1'. The primary variance between CA and BCA is the coot location updating. The initial location of the coot is generated depending on the basic CA and then a probability function is employed to force the coot for choosing either 0 or 1. The probability function is represented in equation (13). The coot's new location is upgraded by adopting the probability function while maintaining the state, as presented in equation (14).

$$T(l_k) = |\tanh(l_k)| \tag{13}$$

$$l_{k\_new} = \begin{cases} \bar{l}_k, & if\ rand \le |T(l_k)| \\ l_k, & otherwise \end{cases} \tag{14}$$

where rand is a random number in the range of [0,1].

The following are the steps of the BCA technique.

Step 1: The algorithm is initialized by resetting population size and iteration.
Step 2: Randomly creates coot locations.
Step 3: Chose leaders randomly from the coot.
Step 4: Evaluate the fitness function.
Step 5: Find the best leader as global optimal.
Step 6: Update the coot location using (14) and evaluate the fitness function.
Step 7: Update the coot location according to the leaders' location, if necessary.
Step 8: Update leaders' location using (14) and evaluate the fitness function.
Step 9: Update global optimum.
Step 10: Repeat Steps 6 to 8 until the iteration criteria are fulfilled.
Step 11: Print the global optimum solution.

4.2.1. Benchmark function

In this study, two mostly used binary algorithm testing benchmark functions are utilized to assess the competence

of BCA. Table 1 shows the properties of binary test functions [38].

Table 1. Binary test functions

ID	Test function	Function name	Search space	Dimension (n)	Best known
F1	$f_1(x)=\sum_{i=1}^{n} x_i$	Max one	$[0,1]^n$	160	160
F2	$f_2(x)=\sum_{i=1}^{\frac{n}{8}}\left(\prod_{j=8(i-1)+1}^{8i} x\right)$	Royal road	$[-5.12,5.12]^n$	160	20

4.2.2. Performance Evaluation

Using binary benchmark functions, the suggested BCA's performance with the bit update technique is evaluated. Additionally, by contrasting the BCA's performance with that of the quantum-inspired binary PSO (QPSO) method, the performance of the BCA is proven [39]. For both strategies, the size of population is set as 30 and the max iteration as 100, respectively.

4.3. Implementation of BCA for MG

The BCA technique is utilized as a controller for maximizing the utilization of solar and wind energy and minimizing the operating cost. In the simulation, BCA generates a binary matrix in which '1' represents the particular generator is ON while '0' represents the particular generator is OFF. In each run, the BCA minimizes the fitness function as shown in equation (15) to reduce the operating cost [25]. Fig.5 illustrates the workflow of BCA for simulating the MG.

$$C_M = (1.5 \times P \times pf \times E_P) \tag{15}$$

where C_M is the minimum cost, P is the power, pf is the power factor and E_P is the energy price \$/MWh per hour.

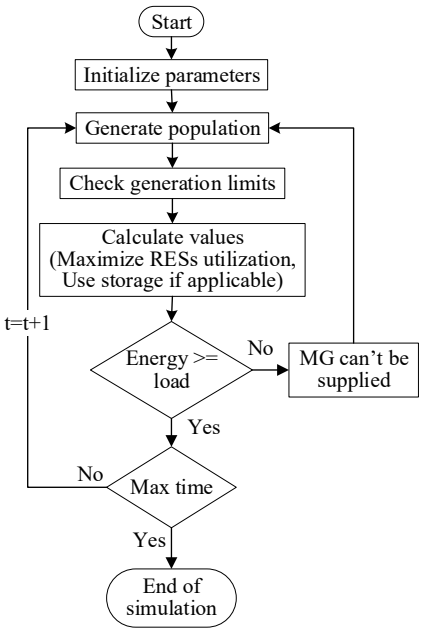

Fig.5. Flow diagram of BCA for the simulation of an MG for 24 hours.

5. Simulation results

5.1. Wind Speed and solar irradiation forecasting

The RF system is optimised utilizing the suggested CA technique. For the purpose of validating the findings, the effectiveness of the recommended approach is evaluated with PSO. Two error indices are used to assess the effectiveness of both strategies. Table 1 displays the predictions made by CA and PSO, whereas Fig. 6 displays how well the optimisation strategies performed in reducing errors. According to the assessment, both approaches can be used to accurately estimate wind speed and solar irradiation. Finding the ideal optimisation method for the RF model is crucial, though. The ideal outcomes of the RF technique with CA are superior to PSO, as seen in Table 2 and Fig. 6.

Table 2. Prediction result for LSA compared with PSO

Prediction technique	Optimization technique	Solar irradiation		Wind speed	
		RMSE	MAPE(%)	RMSE	MAPE(%)
RF	CA	***0.0366***	***2.98***	***0.0602***	***4.78***
	PSO	0.0486	3.81	0.0715	5.93

Note: The bold italic value denotes the minimal error

The CA-based RF projected solar irradiance and wind speed are shown in Fig.7 together with actual data. The anticipated values are unquestionably near to the actual ones, as can be seen from the figure. The RF model makes it easy to predict wind speed and solar radiation, nevertheless, there may be some alterations among the predicted and actual data. The predicted errors of the CA-optimized RF for the dataset on wind speed and solar irradiance are displayed in Fig.8.

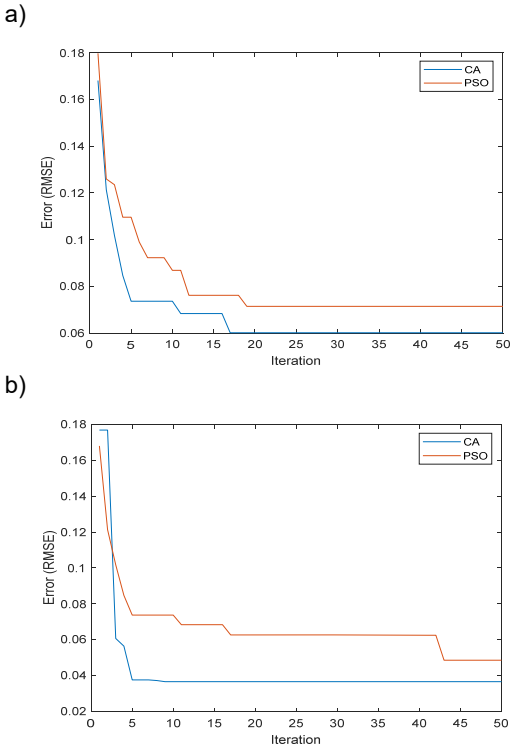

Fig.6. Error minimization for the forecast of (a) wind speed and (b) solar irradiation using CA and PSO

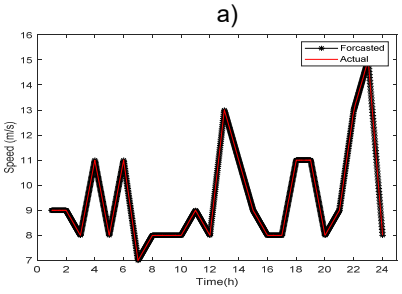

b)

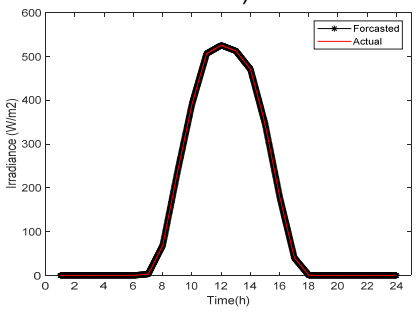

Fig.7. Data on (a) wind speed and (b) solar radiation, both actual and expected, are presented

a)

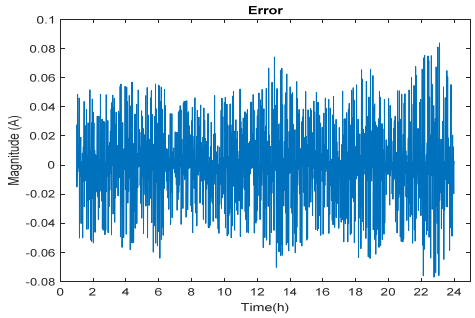

b)

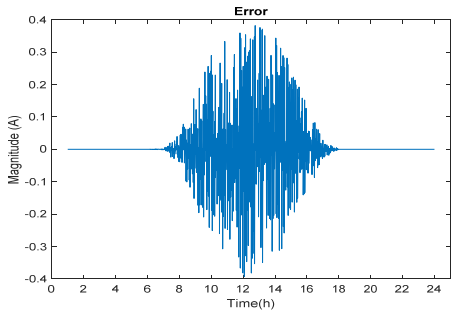

Fig.8. Error curves of (a) wind speed and (b) solar irradiation from a CA optimized RF

5.2. Performance Evaluation of BCA

In this section, the performance of BCA is shown using two binary benchmark functions. Moreover, the performance of BCA is compared with QPSO. Both algorithms are run 30 times for each function to find the consistency and efficiency of the algorithm. Table 3 shows the numerical outcomes and the best performance is indicated in italicized boldface. From the table, it can be shown that both algorithms can find the best solution for F1 and F2. However, the BCA needs a smaller number of iterations to find the best solution. Fig.9 shows the boxplot of 30 independent runs for both F1 and F2. Fig.10 shows the convergence rate curves. From table 3 and figures 9 and 10, it can be concluded that both algorithms can find the best solution, however, BCA performs better than QPSO because this algorithm is more consistent and requires less number of iterations to obtain the best solution

Table 3. Optimization results of benchmark function

ID	Algorithm	Best	Worst	Average	Median	Std. Deviation	Min. iteration
F1	BCA	***160***	***160***	***160***	***160***	***0***	***31***
	QPSO	***160***	157	159.56	***160***	0.7041	205
F2	BCA	***20***	***19***	***19.98***	***20***	***0.1414***	***38***
	QPSO	***20***	17	19.06	19	0.9563	209

a)

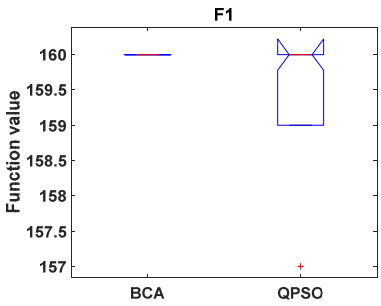

b)

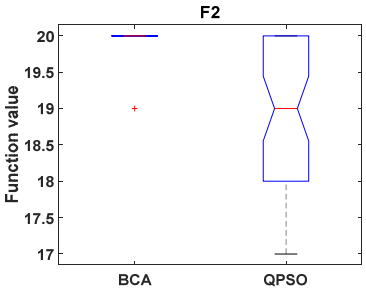

Fig.9. Optimization results of benchmark function. 9(a) F1 and 9(b) F2

a)

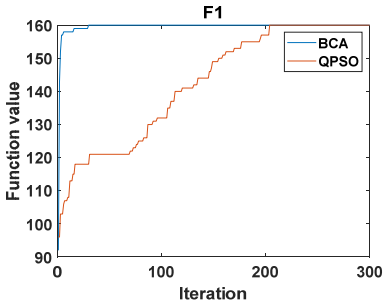

b)

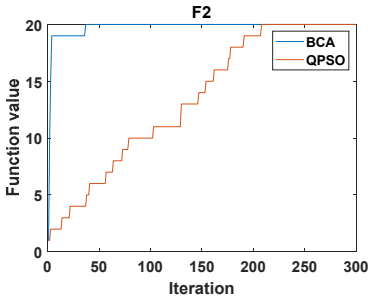

Fig.10. Convergence characteristic curves for BCA and QPSO. 10(a) F1 and 10(b) F2

5.3. Microgrid simulation

In this study, a simulated MG is introduced consisting of a diesel unit, a PV farm, a wind farm, and a battery storage system. Two cases of MG are presented to analyse the power system problems. In the first case, the MG contains a diesel unit, a PV farm, and a wind farm in the simulation. In this case, the energy of the PV and wind systems is fully utilized to reduce the operating cost. The energy generation and demand are considered for a whole day (24 hrs). Fig.11 shows the MG profiles in terms of voltage, current, apparent power, active power, and reactive power for all generations and load demand.

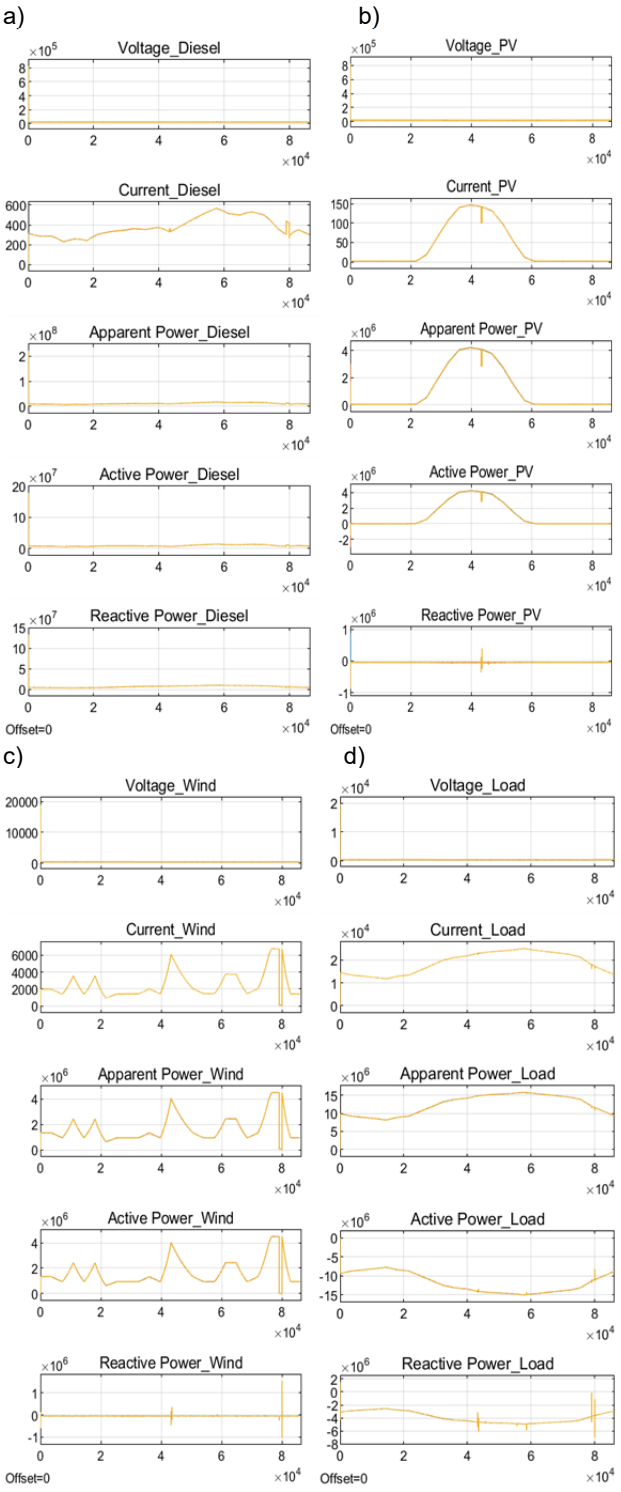

Fig.11. Microgrid profiles for case 1 a) Diesel, b) PV, c) Wind, and d) Load

In the second case, the battery storage system is added to case 1 MG. The battery energy storage system is utilized for specific periods of high load demand to reduce the peak demand. The generation of solar power, wind power, and load demand is the same as in case 1. Similar to case 1, the energy of the PV and wind systems is fully utilized. Fig.11 shows the MG profiles for case 2. From Figures 11 (a) and 12(a), it can be seen that the consumption of diesel power is reduced by introducing a storage system for the peak demand (Fig.12e).

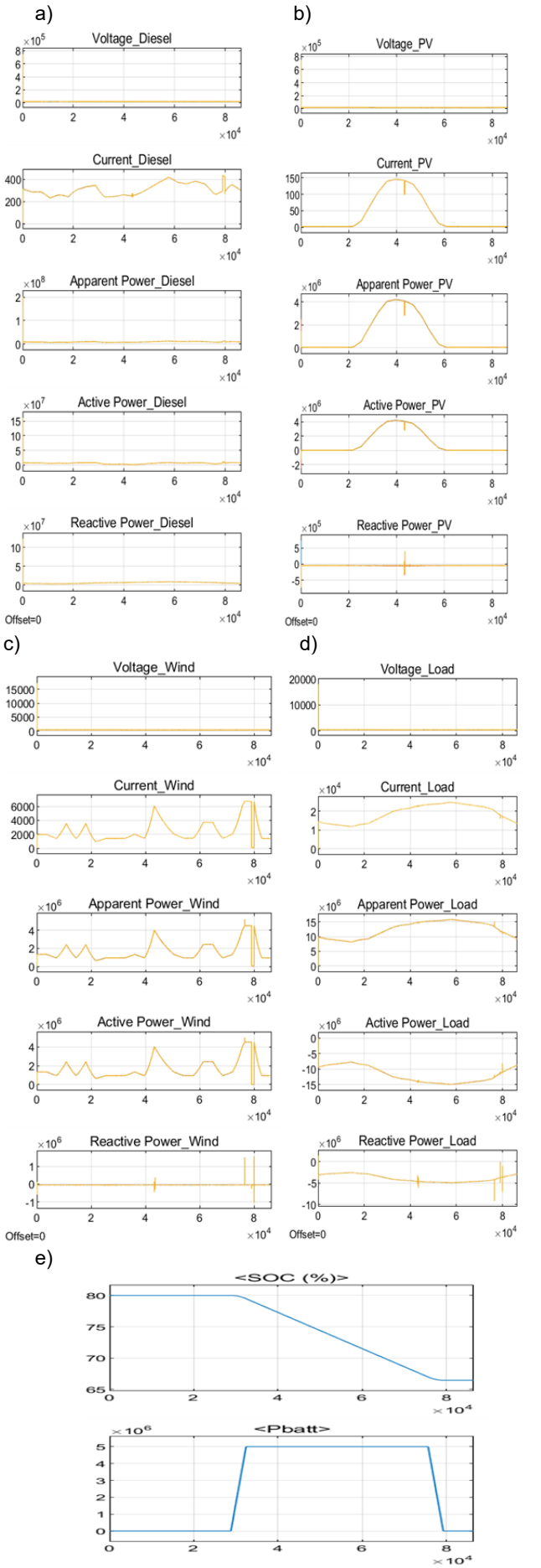

Fig.12. Microgrid profiles for case 2 a) Diesel, b) PV, c) Wind, d) Load, and e) Battery storage

5.4. Cost-effective evaluation

The calculation of operating costs is important for MG. The operating cost of PV and wind farms are cheap, but they are inconsistent in generating power because of the weather conditions. Therefore, a diesel unit is incorporated into the system, but this unit is expensive. Battery storage is enforced to minimize the peak demand. The BCA approach is introduced to optimally schedule the generators to minimize the cost. Energy consumption and electricity cost are calculated per day as follows [25].

$$E(MWh/day) = P(MW) \times t(h/day) \quad (16)$$

$$C_{cost}(\$/day) = E(MWh/day) \times Cost(\$/MWh) \quad (17)$$

where C_{cost} is the energy price/day, P is the active power, E is the energy/day.

The energy cost is calculated for each day. The average tariff rates for renewable energy are varying from 0.04 to 0.10 $/kWh [40]. Fig.13 shows that the cost of a system without battery storage (case 1) is $28328.965, whereas after including battery storage (case 2), the cost reduces to $24407.095.

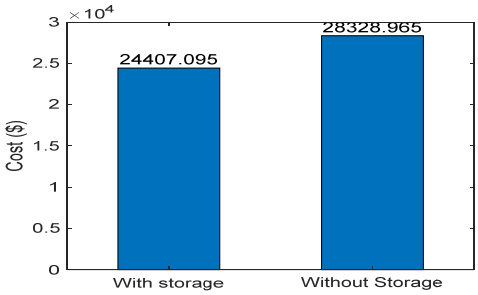

Fig.11. Cost minimization for 24 hours in case of using a storage system

6. Conclusion

The day-to-day average of wind speed and solar radiation is forecasted using an RF algorithm built on deep learning. Additionally, the CA methodology is suggested as a way to enhance the RF forecasting method and reduce forecasting errors. A performance assessment of the proposed CA approach and the familiar PSO algorithm is made. The proposed CA method outperforms the traditional approach in terms of performance. An MG was also designed in MATLAB/SIMULINK using the optimal forecasted data. Two cases are analysed for calculating the operating cost and concluded that the MG with a battery storage system could considerably reduce the operating cost. The prediction model's accuracy will be improved in subsequent work by incorporating large data, according to the scientists. Future work might also include the introduction of the battery storage's bidirectional control.

Acknowledgement

This work was supported in part by the Western Sydney University Grant.

***Authors**: M.Sc. Md Mainul Islam, School of Engineering, Design and Built environment, Western Sydney University, Locked Bag 1797,NSW,2751,Australia,Email:mm.islam@westernsydney.edu.au .Prof. Hussain Shareef, M.Sc. Eslam Salah Fayez Al Hassan, Department of Electrical and Communication Engineering, College of Engineering, United Arab Emirates University, 15551,Al Ain, UAE, E-mail: shareef@uaeu.ac.ae.*

REFERENCES

[1] B. Kumar Sahu, "A study on global solar PV energy developments and policies with special focus on the top ten solar PV power producing countries," *Renewable and Sustainable Energy Reviews,* vol. 43, pp. 621-634, 2015/03/01/ 2015, doi: https://doi.org/10.1016/j.rser.2014.11.058.

[2] M. M. Islam, M. Nagrial, J. Rizk, and A. Hellany, "General Aspects, Islanding Detection, and Energy Management in Microgrids: A Review," *Sustainability,* vol. 13, no. 16, 2021, doi: 10.3390/su13169301.

[3] W. Zhao *et al.*, "A point prediction method based automatic machine learning for day-ahead power output of multi-region photovoltaic plants," *Energy,* vol. 223, p. 120026, 2021/05/15/ 2021, doi: https://doi.org/10.1016/j.energy.2021.120026.

[4] M. W. Zafar, M. Shahbaz, A. Sinha, T. Sengupta, and Q. Qin, "How renewable energy consumption contribute to environmental quality? The role of education in OECD countries," *Journal of Cleaner Production,* vol. 268, p. 122149, 2020/09/20/ 2020, doi: https://doi.org/10.1016/j.jclepro.2020.122149.

[5] D. Zhu, S. M. Mortazavi, A. Maleki, A. Aslani, and H. Yousefi, "Analysis of the robustness of energy supply in Japan: Role of renewable energy," *Energy Reports,* vol. 6, pp. 378-391, 2020/11/01/ 2020, doi: https://doi.org/10.1016/j.egyr.2020.01.011.

[6] V. Gaigalis and V. Katinas, "Analysis of the renewable energy implementation and prediction prospects in compliance with the EU policy: A case of Lithuania," *Renewable Energy,* vol. 151, pp. 1016-1027, 2020/05/01/ 2020, doi: https://doi.org/10.1016/j.renene.2019.11.091.

[7] T. Ahmad, D. Zhang, and C. Huang, "Methodological framework for short-and medium-term energy, solar and wind power forecasting with stochastic-based machine learning approach to monetary and energy policy applications," *Energy,* vol. 231, p. 120911, 2021/09/15/ 2021, doi: https://doi.org/10.1016/j.energy.2021.120911.

[8] S. Goodarzi, H. N. Perera, and D. Bunn, "The impact of renewable energy forecast errors on imbalance volumes and electricity spot prices," *Energy Policy,* vol. 134, p. 110827, 2019/11/01/ 2019, doi: https://doi.org/10.1016/j.enpol.2019.06.035.

[9] D. P. Larson, L. Nonnenmacher, and C. F. M. Coimbra, "Day-ahead forecasting of solar power output from photovoltaic plants in the American Southwest," *Renewable Energy,* vol. 91, pp. 11-20, 2016/06/01/ 2016, doi: https://doi.org/10.1016/j.renene.2016.01.039.

[10] A. Mellit and A. M. Pavan, "A 24-h forecast of solar irradiance using artificial neural network: Application for performance prediction of a grid-connected PV plant at Trieste, Italy," *Solar Energy,* vol. 84, no. 5, pp. 807-821, 2010/05/01/ 2010, doi: https://doi.org/10.1016/j.solener.2010.02.006.

[11] Y. Jiang, "Computation of monthly mean daily global solar radiation in China using artificial neural networks and comparison with other empirical models," *Energy,* vol. 34, no. 9, pp. 1276-1283, 2009/09/01/ 2009, doi: https://doi.org/10.1016/j.energy.2009.05.009.

[12] H. Khorasanizadeh and K. Mohammadi, "Introducing the best model for predicting the monthly mean global solar radiation over six major cities of Iran," *Energy,* vol. 51, pp. 257-266, 2013/03/01/ 2013, doi: https://doi.org/10.1016/j.energy.2012.11.007.

[13] K. Nam, S. Hwangbo, and C. Yoo, "A deep learning-based forecasting model for renewable energy scenarios to guide sustainable energy policy: A case study of Korea," *Renewable and Sustainable Energy Reviews,* vol. 122, p. 109725, 2020/04/01/ 2020, doi: https://doi.org/10.1016/j.rser.2020.109725.

[14] D. Yang, Z. Ye, L. H. I. Lim, and Z. Dong, "Very short term irradiance forecasting using the lasso," *Solar Energy,* vol. 114, pp. 314-326, 2015/04/01/ 2015, doi: https://doi.org/10.1016/j.solener.2015.01.016.

[15] X. Huang *et al.*, "Hybrid deep neural model for hourly solar irradiance forecasting," *Renewable Energy,* vol. 171, pp. 1041-1060, 2021/06/01/ 2021, doi: https://doi.org/10.1016/j.renene.2021.02.161.

[16] J. Wang and Z. Yang, "Ultra-short-term wind speed forecasting using an optimized artificial intelligence algorithm," *Renewable*

Energy, vol. 171, pp. 1418-1435, 2021/06/01/ 2021, doi: https://doi.org/10.1016/j.renene.2021.03.020.
[17] Y. Nie, N. Liang, and J. Wang, "Ultra-short-term wind-speed bi-forecasting system via artificial intelligence and a double-forecasting scheme," *Applied Energy,* vol. 301, p. 117452, 2021/11/01/ 2021,
doi: https://doi.org/10.1016/j.apenergy.2021.117452.
[18] Z. Liu, R. Hara, and H. Kita, "Hybrid forecasting system based on data area division and deep learning neural network for short-term wind speed forecasting," *Energy Conversion and Management,* vol. 238, p. 114136, 2021/06/15/ 2021, doi: https://doi.org/10.1016/j.enconman.2021.114136.
[19] M. Yang, S. Zhu, M. Liu, and W. Lee, "One Parametric Approach for Short-Term JPDF Forecast of Wind Generation," *IEEE Transactions on Industry Applications,* vol. 50, no. 4, pp. 2837-2843, 2014, doi: 10.1109/TIA.2014.2300188.
[20] K. Mason, J. Duggan, and E. Howley, "Forecasting energy demand, wind generation and carbon dioxide emissions in Ireland using evolutionary neural networks," *Energy,* vol. 155, pp. 705-720, 2018/07/15/ 2018,
doi: https://doi.org/10.1016/j.energy.2018.04.192.
[21] S. A. Kalogirou, "Artificial Neural Networks and Genetic Algorithms for the Modeling, Simulation, and Performance Prediction of Solar Energy Systems," in *Assessment and Simulation Tools for Sustainable Energy Systems: Theory and Applications*, F. Cavallaro Ed. London: Springer London, 2013, pp. 225-245.
[22] I. Song, W. Jung, J. Kim, S. Yun, J. Choi, and S. Ahn, "Operation Schemes of Smart Distribution Networks With Distributed Energy Resources for Loss Reduction and Service Restoration," *IEEE Transactions on Smart Grid,* vol. 4, no. 1, pp. 367-374, 2013, doi: 10.1109/TSG.2012.2233770.
[23] M. Falahi, S. Lotfifard, M. Ehsani, and K. Butler-Purry, "Dynamic Model Predictive-Based Energy Management of DG Integrated Distribution Systems," *IEEE Transactions on Power Delivery,* vol. 28, no. 4, pp. 2217-2227, 2013, doi: 10.1109/TPWRD.2013.2274664.
[24] A. Ignat, E. Szilagyi, and D. Petreuş, "Renewable Energy Microgrid Model using MATLAB — Simulink," in *2020 43rd International Spring Seminar on Electronics Technology (ISSE)*, 14-15 May 2020 2020, pp. 1-6, doi: 10.1109/ISSE49702.2020.9120923.
[25] M. G. M. Abdolrasol, M. A. Hannan, A. Mohamed, U. A. U. Amiruldin, I. B. Z. Abidin, and M. N. Uddin, "An Optimal Scheduling Controller for Virtual Power Plant and Microgrid Integration Using the Binary Backtracking Search Algorithm," *IEEE Transactions on Industry Applications,* vol. 54, no. 3, pp. 2834-2844, 2018, doi: 10.1109/TIA.2018.2797121.
[26] R. Nazir, H. D. Laksono, E. P. Waldi, E. Ekaputra, and P. Coveria, "Renewable Energy Sources Optimization: A Micro-Grid Model Design," *Energy Procedia,* vol. 52, pp. 316-327, 2014/01/01/ 2014,
doi: https://doi.org/10.1016/j.egypro.2014.07.083.
[27] S. Chalise, J. Sternhagen, T. M. Hansen, and R. Tonkoski, "Energy management of remote microgrids considering battery lifetime," *The Electricity Journal,* vol. 29, no. 6, pp. 1-10, 2016/07/01/ 2016,
doi: https://doi.org/10.1016/j.tej.2016.07.003.
[28] M. Marzband, E. Yousefnejad, A. Sumper, and J. L. Domínguez-García, "Real time experimental implementation of optimum energy management system in standalone Microgrid by using multi-layer ant colony optimization," *International Journal of Electrical Power & Energy Systems,* vol. 75, pp. 265-274, 2016/02/01/ 2016,
doi: https://doi.org/10.1016/j.ijepes.2015.09.010.
[29] J. Radosavljević, M. Jevtić, and D. Klimenta, "Energy and operation management of a microgrid using particle swarm optimization," *Engineering Optimization,* vol. 48, no. 5, pp. 811-830, 2016/05/03 2016, doi: 10.1080/0305215X.2015.1057135.
[30] M. M. Islam, M. Nagrial, J. Rizk, and A. Hellany, "Dual stage microgrid energy resource optimization strategy considering renewable and battery storage systems," *International Journal of Energy Research,* https://doi.org/10.1002/er.7185 vol. n/a, no. n/a, 2021/08/22 2021, doi: https://doi.org/10.1002/er.7185.
[31] H. Shareef, A. H. Mutlag, and A. Mohamed, "Random Forest-Based Approach for Maximum Power Point Tracking of Photovoltaic Systems Operating under Actual Environmental Conditions," *Computational Intelligence and Neuroscience,* vol. 2017, p. 1673864, 2017/06/15 2017, doi: 10.1155/2017/1673864.
[32] I. Naruei and F. Keynia, "A new optimization method based on COOT bird natural life model," *Expert Systems with Applications,* vol. 183, p. 115352, 2021/11/30/ 2021, doi: https://doi.org/10.1016/j.eswa.2021.115352.
[33] J. Antonanzas, N. Osorio, R. Escobar, R. Urraca, F. J. Martinez-de-Pison, and F. Antonanzas-Torres, "Review of photovoltaic power forecasting," *Solar Energy,* vol. 136, pp. 78-111, 2016/10/15/ 2016,
doi: https://doi.org/10.1016/j.solener.2016.06.069.
[34] "Australian Bureau of Meteorology.." [Online]. Available: http://www.bom.gov.au/jsp/awap/solar/index.jsp?colour=colour&time=latest&step=0&map=solarave&period=month&area=nat.
[35] X. Chen, Z. Y. Dong, K. Meng, Y. Xu, K. P. Wong, and H. W. Ngan, "Electricity Price Forecasting With Extreme Learning Machine and Bootstrapping," *IEEE Transactions on Power Systems,* vol. 27, no. 4, pp. 2055-2062, 2012, doi: 10.1109/TPWRS.2012.2190627.
[36] M. Q. Raza, M. Nadarajah, and C. Ekanayake, "On recent advances in PV output power forecast," *Solar Energy,* vol. 136, pp. 125-144, 2016/10/15/ 2016, doi: https://doi.org/10.1016/j.solener.2016.06.073.
[37] L. Breiman, "Random Forests," *Machine Learning,* vol. 45, no. 1, pp. 5-32, 2001/10/01 2001, doi: 10.1023/A:1010933404324.
[38] M. M. Islam, *Performance comparison of various probability gate assisted binary lightning search algorithm*. Institute of Advanced Engineering and Science (in English), 2019.
[39] Y. Jeong, J. Park, S. Jang, and K. Y. Lee, "A New Quantum-Inspired Binary PSO: Application to Unit Commitment Problems for Power Systems," *IEEE Transactions on Power Systems,* vol. 25, no. 3, pp. 1486-1495, 2010, doi: 10.1109/TPWRS.2010.2042472.
[40] "Renewable Energy Investment in Australia." [Online]. Available: https://www.rba.gov.au/publications/bulletin/2020/mar/pdf/renewable-energy-investment-in-australia.pdf.